Proceedings of the
Annual Stability Conference
Structural Stability Research Council
Toronto, Canada, March 25-28, 2014

Stability and load-carrying capacity of cold-formed steel compression members at elevated temperatures

J.C. Batista Abreu[1], B.W. Schafer[2]

Abstract

The objective of this paper is to explore the strength and design of cold-formed steel (CFS) compression members at elevated temperatures. CFS sections are increasingly used as primary structural members and are required to satisfy all design criteria, including fire demands. Fire resistance of CFS structures is currently insured through adherence to prescriptive building codes and standardized assemblage tests; however, recent research has begun to set the stage for performance-based fire design of CFS structures based on engineering analysis. This study focuses on the load-carrying capacity of CFS compression members at elevated temperatures, succeeding a previous paper on the elastic stability of thin-walled columns under thermal gradients (Batista-Abreu and Schafer 2013). Temperature profiles from heat transfer analysis and mechanical analysis are utilized to estimate the axial capacity of CFS lipped channel sections under simulated fire conditions. Computational simulations include the temperature dependence of material properties, and thermal deformations due to fire, considering thermal gradients through the cross-section of structural members. Elastic buckling analysis is used to evaluate the suitability of the Direct Strength Method (DSM) to predict the load-carrying capacity of CFS compression members at elevated temperatures. DSM-based predictions are compared to a series of results from geometric and material nonlinear analysis with imperfections. Results show that current DSM equations overestimate the axial strength of columns under thermal gradients. An alternative approach consisting of reducing the squash load based on the minimum yield stress in the cross-section is discussed.

1. Introduction

Compared to timber and concrete structures, thin-walled cold-formed steel (CFS) members are potentially more vulnerable to fire effects because of their high surface to volume ratio and relatively high thermal conductivity, potentially causing rapid temperature increase, and consequently a fast stiffness and strength degradation. Under realistic fire conditions and possibly non-uniform temperature distributions, the stiffness and strength vary throughout the section and the length of the member, creating a dynamically changing structural response.

[1] Graduate Research Assistant, Department of Civil Engineering, Johns Hopkins University, <jbatist1@jhu.edu>
[2] Professor and Chair, Department of Civil Engineering, Johns Hopkins University, <schafer@jhu.edu>

Several research groups have investigated the development of design equations based on the Effective Width Method and Direct Strength (DSM) to account for high temperature effects. However, most studies consider a uniform temperature distribution (Kaitila 2002; Chen and Young 2006; Ranawaka and Mahendran 2006; Ranawaka and Mahendran 2010). CFS members are commonly used as load-bearing members in walls assemblies, and in general, CFS studs are sheathed with gypsum boards and surrounded by interior insulation. This configuration results in a heterogeneous temperature distribution during fire action. Non-uniform temperature distributions are likely to be developed throughout the cross-section and along the length of CFS structural members. Consequently, thermal and material properties become non-uniform, producing a complex structural response.

In addition, residual stresses and geometric imperfections influence the behavior of the system. However, residual stresses tend to diminish with increasing temperature (Lee 2004; Ranawaka and Mahendran 2006), and their influence on the compressive ultimate load could be negligible at high temperatures (Gardner and Nethercot 2004; Ellobody and Young 2005; Ranawaka and Mahendran 2010), consistent with findings at ambient temperatures (Schafer and Peköz 1998; Schafer et al. 2010).

In typical models, geometric imperfections are artificially created from buckling modes obtained through linear elastic buckling analysis. According to parametric studies on CFS compression members at elevated temperatures, geometric local imperfections (~t) significantly affect the ultimate strength of short columns (Feng et al. 2004); and global (~L/500) and distortional (~2t) imperfections reduce the ultimate load of long columns at elevated temperatures (Kaitila 2002; Ranawaka and Mahendran 2010). Sensitivity to more realistic imperfections is scarce in the literature. However, recent studies provide the characterization of local, distortional, and global imperfections in CFS members at ambient temperatures (Zeinoddini and Schafer 2012).

Currently, there is no widely recognized design method for CFS compression members with realistic temperature distributions, nor a method that relates load-carrying capacity and fire resistance rating. However, recent studies recognize the advantages of DSM against the traditional effective width method. The existing DSM equations, with reduced mechanical properties, have been found adequate for columns under uniform temperature distributions (Heva et al. 2008; Ranawaka and Mahendran 2009).

Modified DSM curves were proposed by Shahbazian and Wang (2011a, 2011b and 2012) to compute the load-carrying capacity of columns under thermal gradients. In this work, it was found that the design of compression members should include combined axial and moment actions, since thermal bowing and shift of the center of resistance have significant influence on the structural response. The proposed DSM curves correspond to three temperature profiles, assuming that the temperature ratios between the exposed and unexposed flanges are 3.0, 2.0 and 1.5 at 120 minutes. Conclusions of these studies suggest modifications of the local, distortional and global DSM strength curves. The proposed approach also requires the computation of an effective squash load, based on axial load and bending moment interactions.

This paper succeeds a previous paper on the elastic stability of thin-walled columns under thermal gradients (Batista-Abreu and Schafer 2013), and focuses on the load-carrying capacity of

CFS compression members with thermal gradients, including geometric imperfections and residual stresses. The main objective of this study is to judge the feasibility of current DSM equations to be used for fire design of compression members under non-uniform temperature distributions, and explore a simplified approach to predict the axial strength of thin-walled columns through current DSM equations.

2. Computational simulations

The load carrying capacity of CFS compression members was computed through shell finite element collapse analysis (i.e. geometric and material nonlinear analysis on the imperfect member) in Abaqus (ABAQUS 2013) and by DSM equations. The cross-section analyzed in this study corresponds to a thin-walled cold-formed steel lipped channel designated as a 400S200-54 (SSMA 2011, AISI-S200-12), with dimensions as shown in Fig. 1. In total, 360 finite element models were analyzed, considering two temperature profiles at multiple times of fire exposure, with lengths varying from 4 in. (101.6 mm) to 96 in. (2438.4 mm), pinned end conditions, and residual stresses and geometric imperfections as described herein.

2.1 Temperature distributions

The non-uniform temperature distribution on the thin-walled studs were obtained through thermal analysis and validated experimentally by Feng et al. (2003b). Two temperature profiles for lipped channels presented in Feng et al. (2003a) were used to simulate the fire action on the structural members, as shown in Figs. 2 and 3. Temperature profile 1 resulted from fire exposure on one side of a CFS wall with a single layer of gypsum board sheathing, while temperature profile 2 was obtained from a similar system with a double layer of gypsum board sheathing. Temperature profile 1 shows higher temperatures over time compared to temperature profile 2 (Fig. 4), thus it is expected to provoke faster degradation of the load-carrying capacity of the structural members.

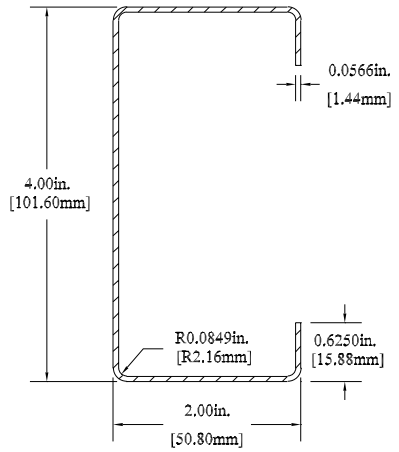

Figure 1: Section 400S200-54 dimensions (SSMA 2011, AISI-S200-12)

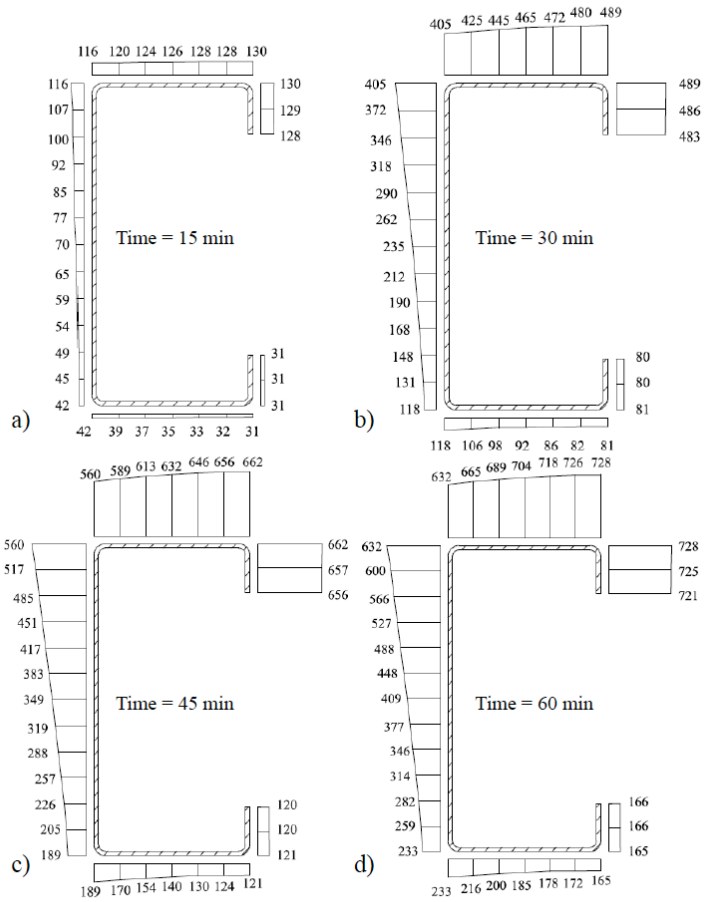

Figure 2: Temperature profile 1 - CFS wall with single layer of gypsum board sheathing exposed to the standard fire curve on one side, from (Feng et al. 2003)

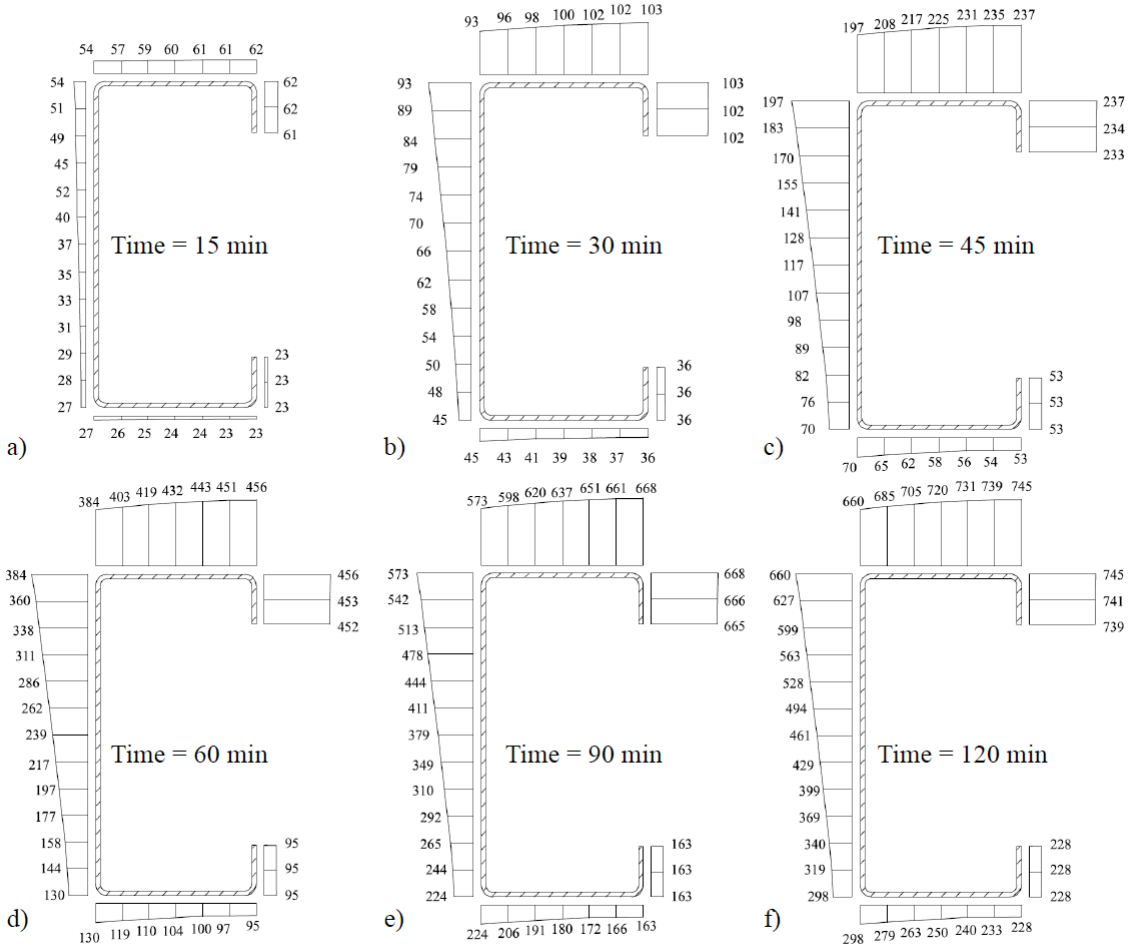

Figure 3: Temperature profile 2 - CFS wall with double layers of gypsum board sheathing exposed to the standard fire curve on one side, from (Feng et al. 2003)

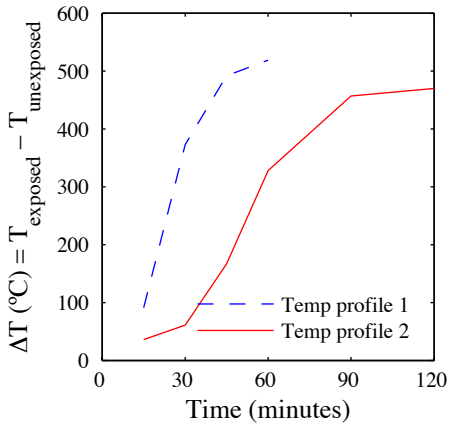

Figure 4: Temperature difference between exposed and unexposed flanges of a 400S200-54 stud over time, for temperature profiles 1 and 2

2.2 Mechanical properties

Computational models included the degradation of the strength and stiffness according experimental results on CFS specimens from Kankanamge and Mahendran (2011), and minor variations of the Poisson's ratio and thermal expansion coefficient from Luecke et al. (2005) and Eurocode 3: Part 1-2 (2005), respectively (Fig. 5). Temperature-dependent true stress versus plastic true strain curves computed from engineering stress-strain prediction equations from Kankanamge and Mahendran (2011) are shown in Fig. 6 and are utilized in the analysis.

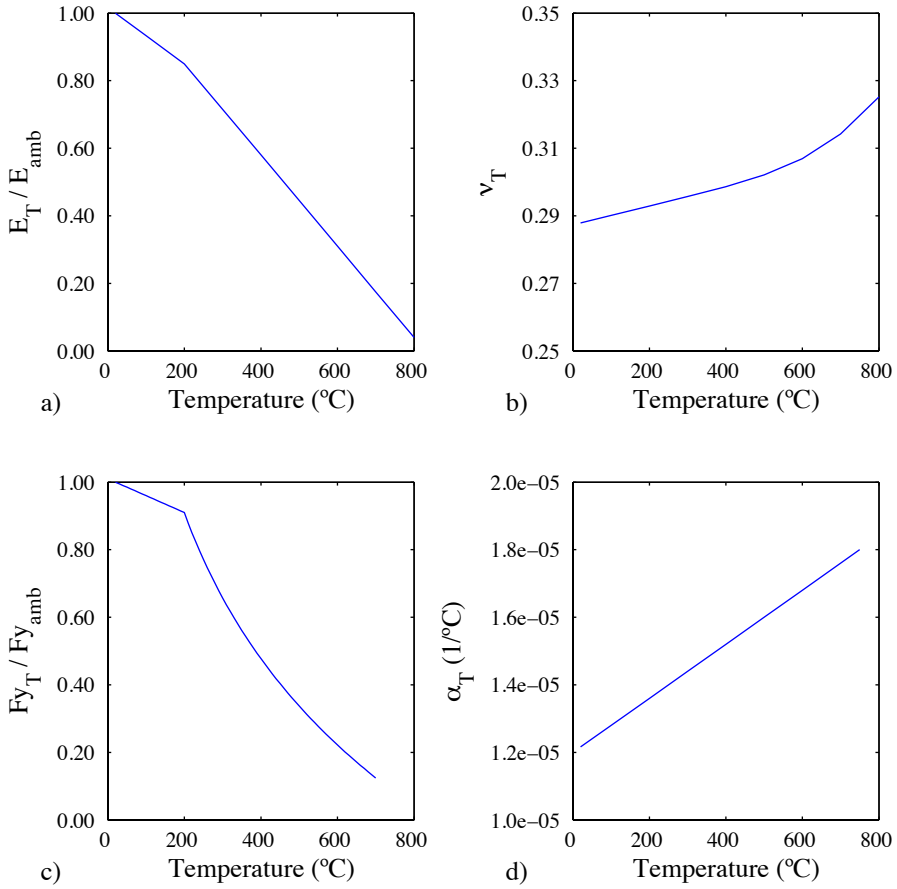

Figure 5: Mechanical properties of steel at elevated temperatures. (a) Retention factor for the elastic modulus (Kankanamge and Mahendran 2011), (b) Poisson's ratio (Luecke, McColskey et al. 2005), (c) retention factors for the yield stress (Kankanamge and Mahendran 2011), and (d) thermal expansion coefficient (Eurocode 3: Part 1-2, 2005)

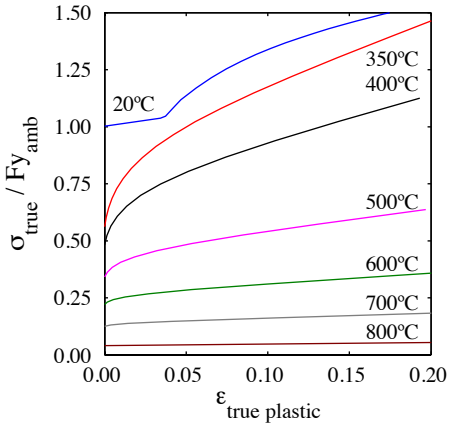

Figure 6: Normalized true stress versus plastic true strain from (Kankanamge and Mahendran 2011)

2.3 Geometric imperfections and residual stresses and strains

Initial geometric imperfections were modeled based on superposition of elastic buckling modes with magnitudes proposed by (Zeinoddini and Schafer 2012). The statistical values for local, distortional, and global imperfection magnitudes are provided in Table 1.

Residual stresses and strains were determined from the mechanics-based method proposed by (Moen et al. 2008). The prediction method suggests only corner residual stresses and plastic strains need to be considered. Residual stresses in the flat parts of the 400S200-54 can be ignored due to relatively large yield stress (345 MPa or 50 ksi) and small thickness (0.0566 in. or 1.44 mm). Effective strains and residual stresses included in the finite element models (FEM) are shown in Fig. 7. The statistical mean of the coil radius (i.e. 474 mm) was assumed in the calculations. Due to corner bending, a maximum true plastic strain of 25% was included.

Quadrilateral shell elements with nine nodes and five degrees of freedom per node (S9R5), with thirty-one through-thickness integration points were used in the simulations. The inclusion of residual stresses and plastic strains in the analysis results in a slight increase in the load-carrying capacity of the CFS column (up to 7.6% for 400S200-54 columns with temperature profile 2, at 60 minutes). However, their effect is less significant as the slenderness of the member increases, which is the case of long columns or members subjected to very high temperatures (Fig. 8-a).

Collapse analyses with several imperfection magnitudes were performed, considering temperature profile 2, at 60 minutes of fire exposure (Fig. 8-b). Compared to the cases with imperfection magnitudes corresponding to the 50th percentile, the axial capacity of members with imperfection magnitudes in the 25th percentile resulted in at most 7.1% higher loads. In contrast, the axial capacity of members with imperfections corresponding to the 75th and 95th percentiles resulted in, at most, 7.5% and 17.9% lower loads, respectively. Consistent with the ambient case, results indicate the larger the imperfections the lower the axial capacity of compression members – and this reality holds with temperature. Imperfection magnitudes of the 50th percentile are used in the following simulations.

Table 1. Imperfection magnitudes from Zeinoddini and Schafer (2012)

Case	Local (δ_o/t)	Distortional (δ_o/t)	Bow (L/δ_o)	Camber (L/δ_o)
25th percentile	0.17	0.43	4755	6295
50th percentile	0.31	0.75	2909	4010
75th percentile	0.54	1.14	1659	2887
95th percentile	1.02	3.06	845	1472

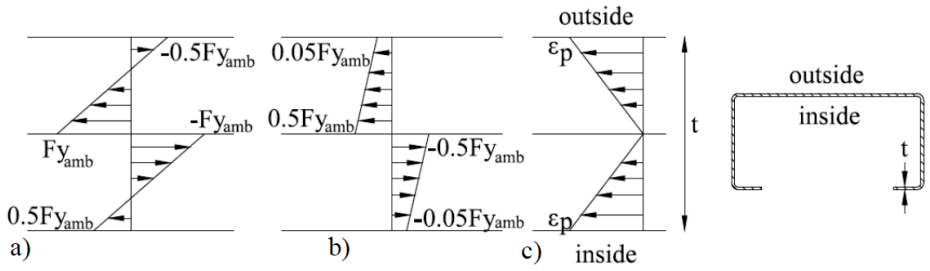

Figure 7: Residual stresses in the (a) transverse and (b) longitudinal directions, and (c) effective plastic strains in corner regions of thin-walled members

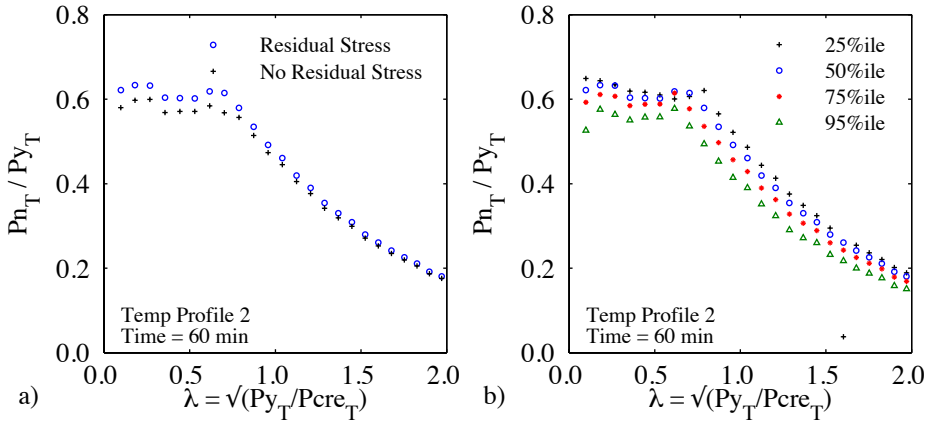

Figure 8: Strength curves for 400S200-54 columns under temperature profile 2, at 60 minutes of fire exposure. Variation of column strength with (a) residual stresses, and (b) imperfection magnitudes

3. Results from GMNIA and DSM

The nominal axial capacity of compression members was computed through shell finite element collapse (GMNIA) analysis and compared with DSM predictions. For DSM, elastic buckling loads (i.e. local, distortional, and global) were computed through CUFSM (Li and Schafer 2010). Temperature dependent material properties were included in the finite strip analysis. The temperature-dependent squash load was computed assuming a weighted average yield stress (Fy_T), or using the minimum yield stress of the cross-section (Fy_{min}). Following the temperature distribution of profiles 1 and 2, the squash load degrades over time (Fig. 9-a). Simultaneously, the slenderness of columns, even at the same physical length, increases with temperature (over time), since the degradation of the elastic buckling load governs the response (Fig. 9-b). In other words, columns become more slender and have a lower squash load as temperature (time) increases. This fact is reflected in typical DSM slenderness vs. strength curves: a point of the curve corresponding to a structural member with a specific geometry (cross-section and length) moves "down" losing load-carrying capacity, and to the "right" becoming more slender, as the temperature (time) increases.

At ambient temperature, results from GMNIA collapse analysis and DSM are comparable (Fig. 10) as expected. However, at elevated non-uniform temperatures, DSM (used only with simple changes) overestimates the load-carrying capacity of the compression members, at least in part due to thermal bowing and other factors not considered in the analysis. Figs. 11 and 12 shows the column strength curves of members with temperature distributions based on profiles 1 and 2, respectively. The plots show the strength of columns is reduced and their slenderness is increased as time elapses (and temperature increases). Fig. 13 shows the failure mode of the columns becomes unsymmetrical due to non-uniform material strength and stiffness, and modal interactions are more pronounced (Batista Abreu and Schafer 2013).

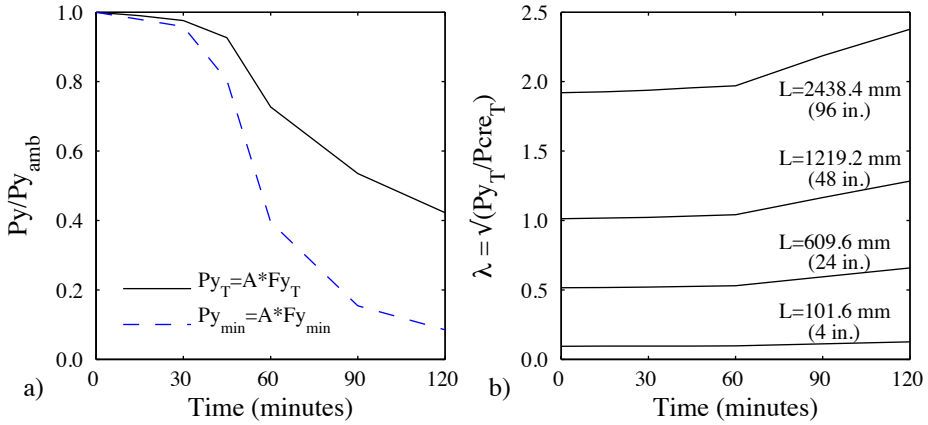

Figure 9: Variation of the (a) squash load computed with average (Fy_T) and minimum (Fy_{min}) yield stresses, and (b) slenderness of columns with temperature profile 2

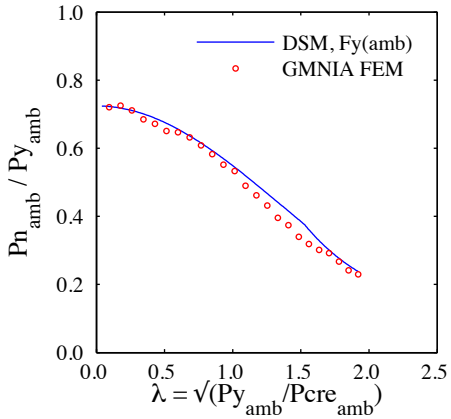

Figure 10: Column strength curve at ambient temperature

An alternative DSM approach to estimate the nominal axial strength of CFS columns consists in computing the squash load as the product of the cross-sectional area and the minimum yield stress of the section (Fy_{min}). This is similar in spirit to using first yield in bending (M_y) instead of the fully plastic bending moment (M_p). This reduced squash load (Py_{min}) is then used in DSM equations to estimate the load-carrying capacity of columns. Although this approach penalizes the overall yield strength of the member, results show the predicted axial capacity is only modestly conservative compared to collapse analysis results (Figs. 14 and 15). However, if this criterion were utilized to compute the slenderness of the column, equations would suggest

slenderness ratios less than the actual values. Essentially, this approach allows the yielding failure to have a more dominant role in the prediction of the structural response.

DSM results based on squash load derived from the minimum yield stress (Py_{min}) are presented in Figs. 16 and 17, and compared to GMNIA collapse analysis results. Normalization of the axial strength and slenderness ratios are based on ambient temperature conditions. The degradation of the axial strength with increasing temperature is not proportional among members with different physical lengths (or ambient slenderness) since failure modes evolve while temperature increases. However, in all cases the axial strength predicted by current DSM equations are similar to results form GMNIA.

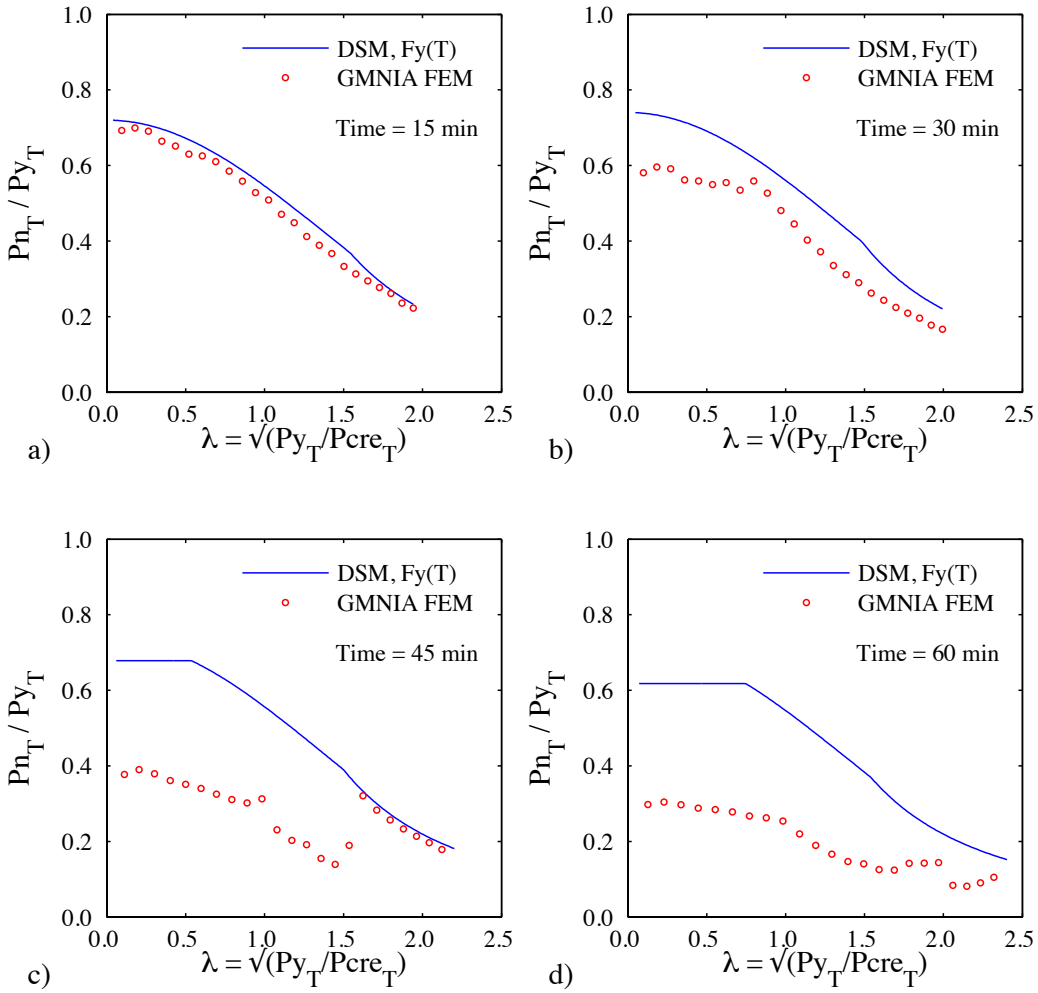

Figure 11: DSM predictions based on weighted average squash load (Py_T) and GMNIA results normalized with weighted average squash load (Py_T), corresponding to temperature profile 1

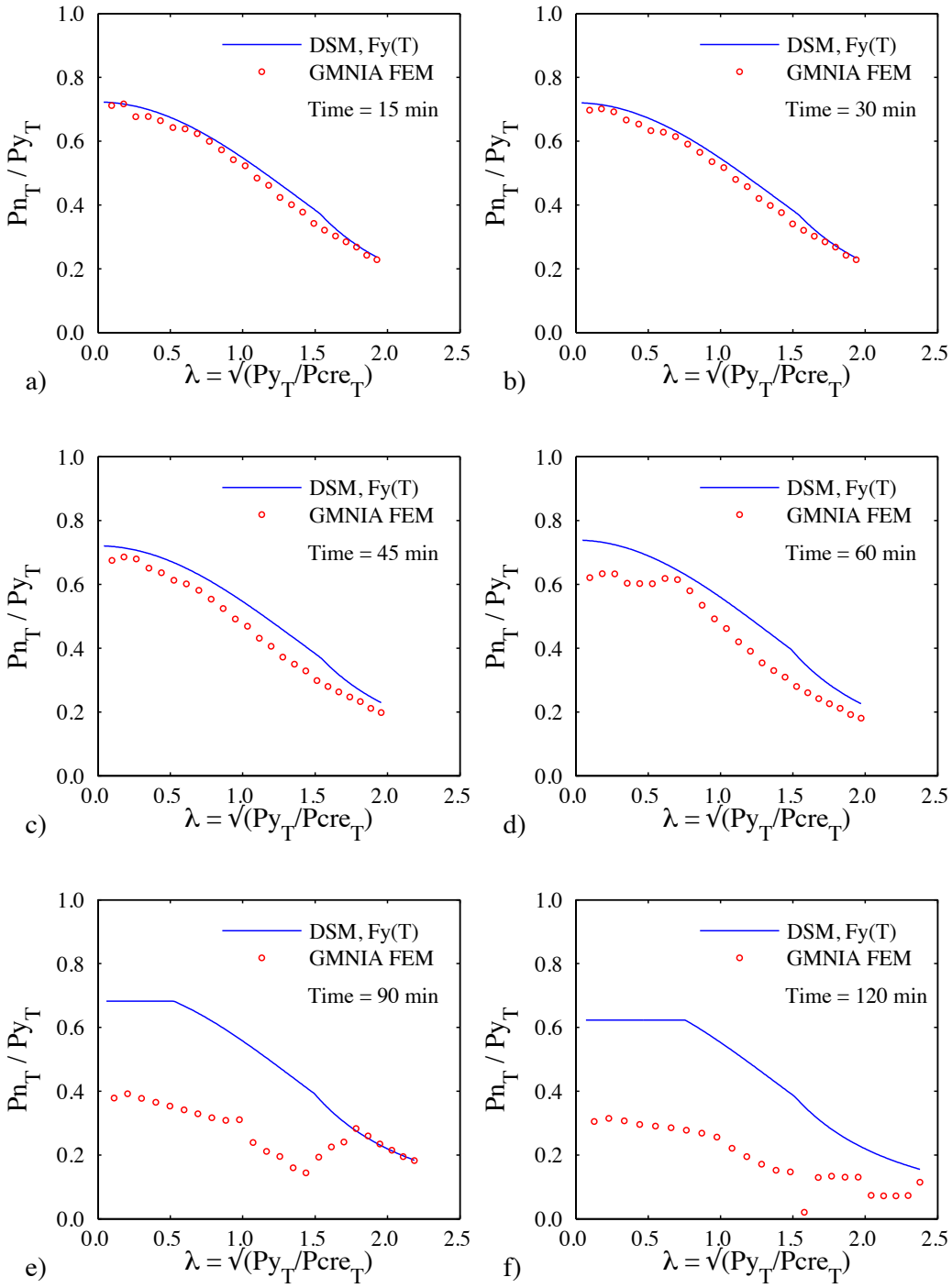

Figure 12: DSM predictions based on weighted average squash load (PyT) and GMNIA results normalized with weighted average squash load (PyT), corresponding to temperature profile 2

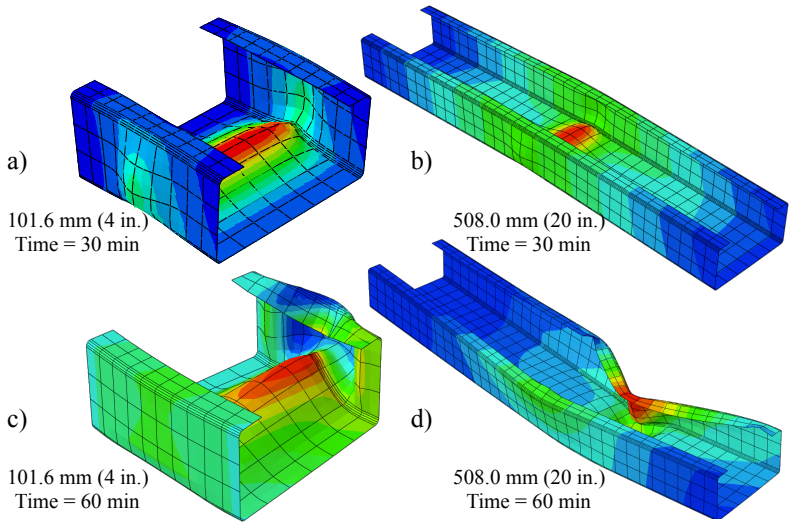

Figure 13: Deformed shapes of CFS columns with temperature profile 2. 101.6 mm (4 in.) long columns at (a) 30 minutes and (b) 60 minutes, and 508.0 mm (20 in.) long columns at (c) 30 minutes and (d) 60 minutes of fire exposure

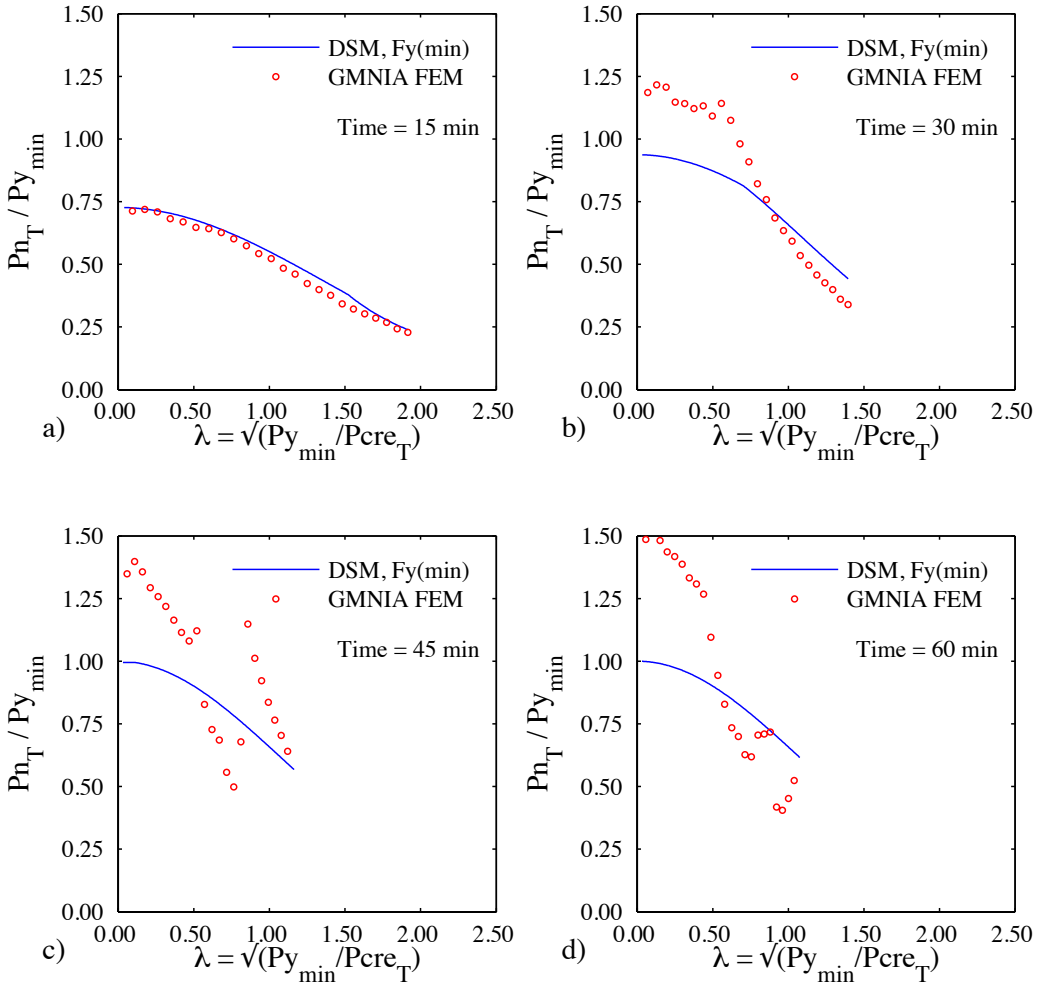

Figure 14: DSM predictions based on minimum squash load ($A_g \times Fy_{min}$) and GMNIA results normalized with minimum squash load ($A_g \times Fy_{min}$), corresponding to temperature profile 1

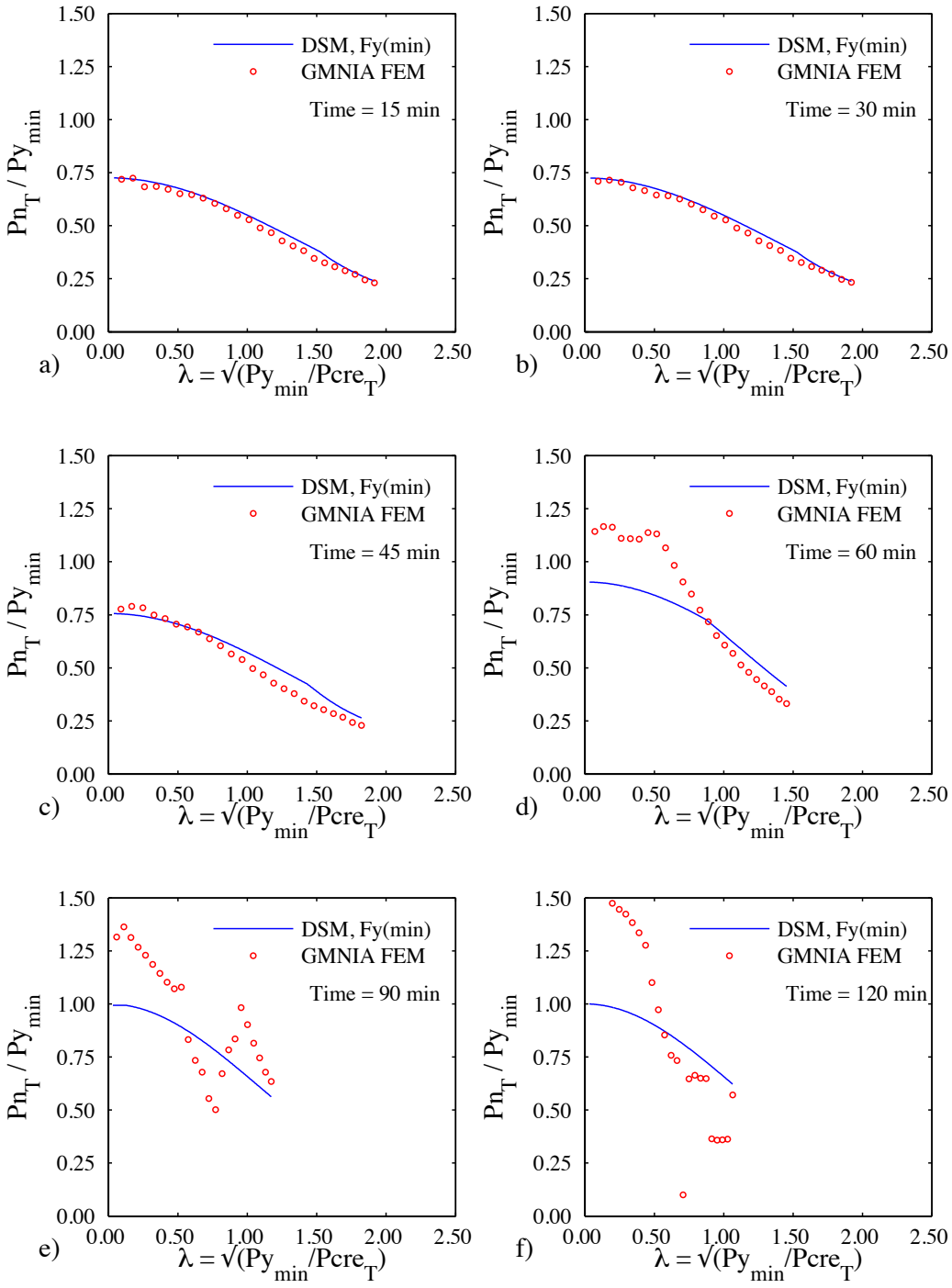

Figure 15: DSM predictions based on minimum squash load ($A_g \times Fy_{min}$) and GMNIA results normalized with minimum squash load ($A_g \times Fy_{min}$), corresponding to temperature profile 2

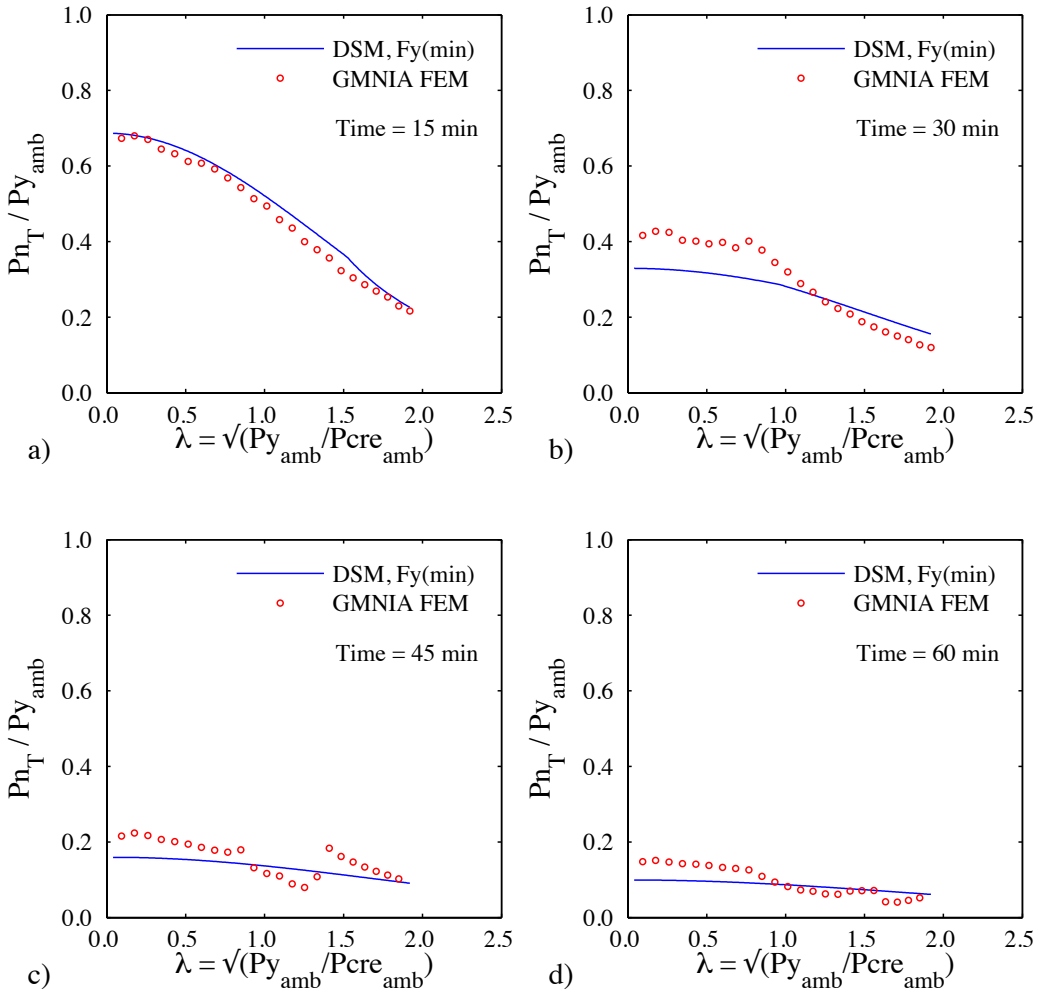

Figure 16: DSM predictions based on minimum squash load ($A_g \times Fy_{min}$) and GMNIA results normalized with ambient squash load ($A_g \times Fy_{amb}$), corresponding to temperature profile 1

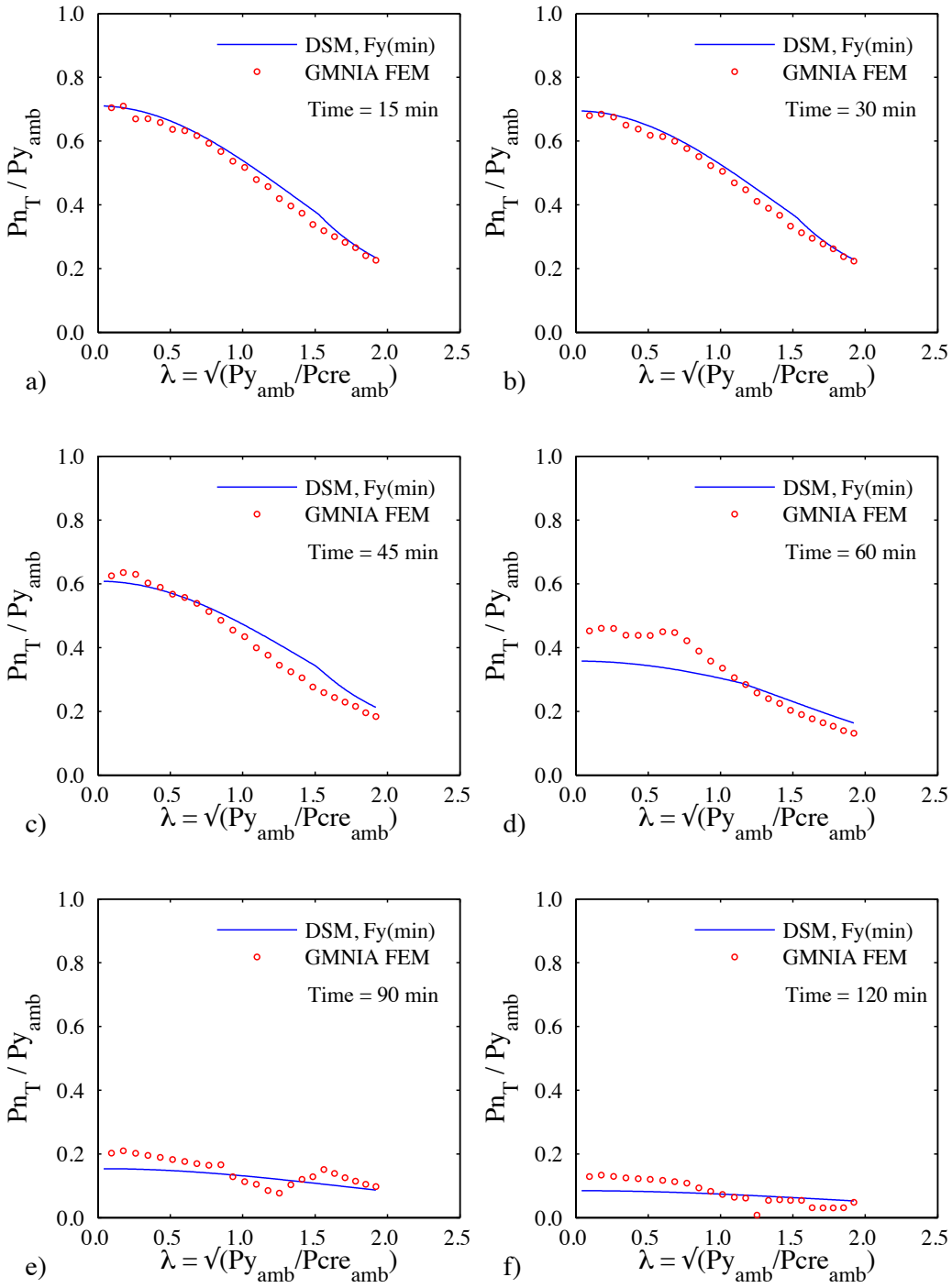

Figure 17: DSM predictions based on minimum squash load ($A_g \times Fy_{min}$) and GMNIA results normalized with ambient squash load ($A_g \times Fy_{amb}$), corresponding to temperature profile 2

4. Conclusions

This paper studies the degradation of the axial strength of cold-formed steel compression members under thermal gradients, based on temperature profiles from heat transfer analysis developed from experimental tests. Geometric and material nonlinear shell finite element analysis with imperfections is used to evaluate the structural behavior of cold-formed steel structural studs subjected to simulated fire conditions. Results show that cold-formed steel columns lose strength and become more slender with increasing temperature due to degradation of mechanical properties and thermal deformations. Final collapse is unsymmetric, exhibits noticeable minor-axis bending due to thermal bowing, and includes coupled buckling modes. Comparisons of the results with the Direct Strength Method are completed. Elastic stability is established at a specific time (t) for a given temperature profile (T) around the section through computational finite strip analysis. Two methods are considered for establishing the squash load, one uses a weighted average: $Py_T=\Sigma A_i Fy_i(t,T)$ and considers the variation around the section; and the second simply uses the minimum yield stress: $Py_{min}=A_g \times \min(Fy(t,T))$. The Direct Strength Method equations (coefficients etc.) are not modified. The weighted average approach (Py_T) is rational, but leads to unconservative strength predictions. The minimum squash load method (Py_{min}) is shown to provide modestly conservative solutions across the study, and is simple to apply. Additional work remains to explore coupled heat transfer analysis, varied members and boundary conditions (for both heat transfer and structural response), and the impact of coupled modes in the response.

Acknowledgments

The authors wish to thank Baofeng Zheng for his help in developing the Matlab code for generating the Abaqus input files.

References

American Iron and Steel Institute, "AISI Standard, AISI S100-2007. North American Specification for the Design of Cold-formed Steel Structural Members." American Iron and Steel Institute, Washington DC.

European Committee for Standardization (CEN). "Eurocode 3: Design of steel structures. Part 1-2: General rules. Structural fire design." Brussels, 2005.

ABAQUS (2013). "ABAQUS 6.13 Documentation." Providence, RI, USA.

Batista-Abreu, J. C. and B. W. Schafer (2013). "Stability of cold-formed steel compression members under thermal gradients." *Annual Stability Conference Structural Stability Research Council,* St. Louis, MO.

Chen, J. and B. Young (2006). "Design of cold-formed steel lipped channel columns at elevated temperatures." *Stability and ductility of steel structures*. Lisbon, Portugal.

Ellobody, E. and B. Young (2005). "Structural performance of cold-formed high strength stainless steel columns." *Journal of Constructional Steel Research,* 61(12): 1631-1649.

Feng, M., Y. C. Wang, et al. (2003a). "Axial strength of cold-formed thin-walled steel channels under non-uniform temperatures in fire." *Fire Safety Journal* 38(8): 679-707.

Feng, M., Y. C. Wang, et al. (2003b). "Thermal performance of cold-formed thin-walled steel panel systems in fire." *Fire Safety Journal,* 38(4): 365-394.

Feng, M., Y. C. Wang, et al. (2004). "A numerical imperfection sensitivity study of cold-formed thin-walled tubular steel columns at uniform elevated temperatures." *Thin-Walled Structures* 42(4): 533-555.

Gardner, L. and D. Nethercot (2004). "Numerical Modeling of Stainless Steel Structural Components—A Consistent Approach." *Journal of Structural Engineering,* 130(10): 1586-1601.

Heva, B., D. Yasintha, et al. (2008). "Local Buckling Tests of Cold-formed Steel Compression Members at Elevated Temperatures." *5th International Conference on Thin-walled Structures - ICTWS 2008*: *Innovations in Thin-walled Structures*. Gold Coast, Australia: 745-752.

Kaitila, O. (2002). "Finite element modelling of cold-formed steel members at high temperatures." Department of Civil and Environmental Engineering. Espoo, Finland, Helsinki University of Technology. Licentiate of Science in Technology.

Kankanamge, N. D. and M. Mahendran (2011). "Mechanical properties of cold-formed steels at elevated temperatures." *Thin-Walled Structures,* 49(1): 26-44.

Lee, J. H. (2004). "Local buckling behaviour and design of Cold-formed steel compression members at elevated temperatures". School of Civil Engineering, Queensland University of Technology. Doctor of Philosophy: 347.

Li, Z. and B. W. Schafer (2010). "Buckling analysis of cold-formed steel members with general boundary conditions using CUFSM: conventional and constrained finite strip methods." *Twentieth International Specialty Conference on Cold-Formed Steel Structures,* Saint Louis, MO.

Luecke, W. E., J. D. McColskey, et al. (2005). "Mechanical Properties of Structural Steels (Draft). Federal Building and Fire Safety Investigation of the World Trade Center Disaster. NIST NCSTAR 1-3D (Draft)". U.S. Deprtment of Commerce. Washington, DC. Government Printing Office.

Moen, C. D., T. Igusa, et al. (2008). "Prediction of residual stresses and strains in cold-formed steel members." *Thin-Walled Structures,* 46(11): 1274-1289.

Ranawaka, T. and M. Mahendran (2006). "Finite element analyses of cold-formed steel columns subject to distortional buckling under simulated fire conditions." *Stability and ductility of steel structures*. Lisbon, Portugal.

Ranawaka, T. and M. Mahendran (2009). "Distortional buckling tests of cold-formed steel compression members at elevated temperatures." *Journal of Constructional Steel Research,* 65(2): 249-259.

Ranawaka, T. and M. Mahendran (2010). "Numerical modelling of light gauge cold-formed steel compression members subjected to distortional buckling at elevated temperatures." *Thin-Walled Structures,* 48(4-5): 334-344.

Schafer, B. W., Z. Li, et al. (2010). "Computational modeling of cold-formed steel." *Thin-Walled Structures,* 48(10–11): 752-762.

Schafer, B. W. and T. Peköz (1998). "Computational modeling of cold-formed steel: characterizing geometric imperfections and residual stresses." *Journal of Constructional Steel Research,* 47(3): 193-210.

Shahbazian, A. and Y. C. Wang (2011a). "Application of the Direct Strength Method to local buckling resistance of thin-walled steel members with non-uniform elevated temperatures under axial compression." *Thin-Walled Structures,* 49(12): 1573-1583.

Shahbazian, A. and Y. C. Wang (2011b). "Calculating the global buckling resistance of thin-walled steel members with uniform and non-uniform elevated temperatures under axial compression." *Thin-Walled Structures,* 49(11): 1415-1428.

Shahbazian, A. and Y. C. Wang (2012). "Direct Strength Method for calculating distortional buckling capacity of cold-formed thin-walled steel columns with uniform and non-uniform elevated temperatures." *Thin-Walled Structures,* 53(0): 188-199.

SSMA (2011). "Product Technical Information." Steel Stud Manufacturers Association.

Zeinoddini, V. M. and B. W. Schafer (2012). "Simulation of geometric imperfections in cold-formed steel members using spectral representation approach." *Thin-Walled Structures,* 60(0): 105-117.